

The contribution of robotic telescopes to the knowledge of our Universe

F. Giovannelli

*INAF - Istituto di Astrofisica e Planetologia Spaziali (E-mail:
franco.giovannelli@iaps.inaf.it)*

Received: June 25, 2023; Accepted: September 6, 2023

Abstract. In this review I will discuss the importance of small telescopes for the advancement of knowledge of our Universe. The use of robotic telescopes scattered all over the world is fundamental. The results obtained complement those obtained with medium and large telescopes and with both small and large space experiments. Due to the limited space and my limited knowledge I will be forced to discuss some topics, important in my opinion, but which obviously do not pretend to permeate the entire field of astrophysics.

Key words: GRBs – SNe – Optical Transients – HE-Astrophysics – Exoplanets

1. Introduction

One of the most important problems in modern astrophysics is that of the long surveys of different kind of cosmic sources. For this purpose the medium and large telescopes are practically unuseful since their allocated time is restricted by the numerous excellent programs that allow only to short periods of scheduling. Thanks to the modern CCD cameras placed in the focus of small telescopes, not subject to limited scheduled time, it is possible to operate for long term surveys up to ~ 21 - 22 mag. Of course a limitation is coming from the lack of observers that for different reasons cannot operate continuously. Thus, the winner idea of using robotic telescopes was used starting from about three decades ago.

Robotic telescopes have many advantages. Removing humans from the observing process allows faster observation response times. Robotic telescopes can also respond quickly to alert broadcasts from satellites and begin observing within seconds. Particularly in the field of gamma ray bursts, very early observations have led to significant advances in astronomers understanding of these events. Automation in a telescopes observing program eliminates the need for an observer to be constantly present at a telescope. This makes observations more efficient and less costly. Many telescopes operate in remote and extreme environments such as mountain tops, deserts, and even Antarctica. Under difficult conditions like these, a robotic telescope is usually cheaper, more reliable and more efficient than an equivalent non-robotic telescope.

However, the main disadvantage of a robotic system is that automation requires work. The more sophisticated the degree of autonomy the telescope has, the greater the amount of work required to enable that functionality. Scheduling systems usually combine a number of different variables (visibility, priority, weather conditions and many more) in order to decide the best course of action for a telescope at any given time (based on work by Eric Saunders, Las Cumbres Observatory: <https://lco.global/spacebook/telescopes/robotic-telescopes/>).

Among the many fields of astrophysics that can be explored with the aid of small telescopes, there is one particularly important: the detection of exoplanets. For this purpose there are different methods for their detection, namely: (i) Radial velocities method (Wright, 2018); (ii) Transit photometry method (Deeg & Roj, 2018); (iii) Gravitational microlensing method (Batista, 2018); (iv) Astrometry method (Malbet & Sozzetti, 2018); (v) Direct imaging method (Pueyo, 2018); (vi) Timing method (pulsars and stellar pulsations) (Kramer, 2018 and Hermes, 2018, respectively); (vii) Radio observations method (Lazio, 2018).

Bennett et al. (2019) in "*Astro2020 Science White Paper*" summarize current and planned exoplanet detection programs using a variety of methods.

Yee et al. (2018) in "*White Paper: Exoplanetary Microlensing from the Ground in the 2020s*" discussed on Microlensing that can access planet populations that no other method can probe: cold wide-orbit planets beyond the snow line^(*), planets in both the Galactic bulge and disk, and free floating planets (FFPs). The demographics of each population will provide unique constraints on planet formation.

It is important to mention the PhD thesis of Clément Ranc (2015a) "*Exoplanets and brown dwarfs detections through gravitational microlensing. Study of interferometric observations*". He discussed the gravitational microlensing effect that has become a unique tool to detect and characterise exoplanets. A microlensing effect occurs when a foreground star (the microlens) and a background star (the source) are aligned with the Earth on the same line of sight. The light from the furthest star, usually in the Galactic bulge, is deflected by the microlens located on the disk. During this phenomenon, multiple images of the source are created by the lens, bigger than the source that consequently seems amplified. When one of these images are located in the vicinity of an exoplanet, a short amplification jump occurs revealing its presence. After a quick overview of the exoplanets field of research, he highlighted the specificities of microlensing comparing to the other planets detection techniques.

^(*) Snow line or ice line or frost line, is the particular distance in the solar nebula from the central protostar where it is cold enough for volatile compounds such as water, ammonia, methane, carbon dioxide, and carbon monoxide to condense into solid ice grains (i.e., for the water, it is the minimum radius from the Sun at which water ice could have condensed, at about 150 K (-190 °F, -120 °C) (e.g. Liu, Yao & Ding (2017)).

2. A summary of the robotic experiments

In this short excursion about the tools necessary for an advance of our knowledge of the physics of the Universe, we cannot omit the extreme importance of small experiments, like those Space-based: small-, mini-, micro-, nano-, and cube-satellites, and those Ground-based: small-telescope, and Robotic-telescopes.

Castro-Tirado (2010a) in his review "*Robotic Autonomous Observatories: A Historical Perspective*" presented a historical introduction to the field of Robotic Astronomy, discussing the basic definitions, the differing telescope control operating systems, observatory managers, as well as a few current scientific applications in that time.

The number of automatic astronomical facilities worldwide continues to grow, and the level of robotisation, autonomy, and networking is increasing as well. This has a strong impact in many astrophysical fields, like the search for extrasolar planets, the monitoring of variable stars in our Galaxy, the study of active galactic nuclei, the detection and monitoring of supernovae, and the immediate followup of high-energy transients such as gamma-ray bursts (Castro-Tirado, 2008, 2010b).

The number of Robotic Autonomous Observatories (RAOs) has rapidly grown. Figure 1 shows the location of more than 100 RAOs worldwide (Castro Cerón, 2011). They are providing excellent results which should be impossible to obtain with the larger telescopes subject to strict scheduling, and in any case not available for long term runs of observations.

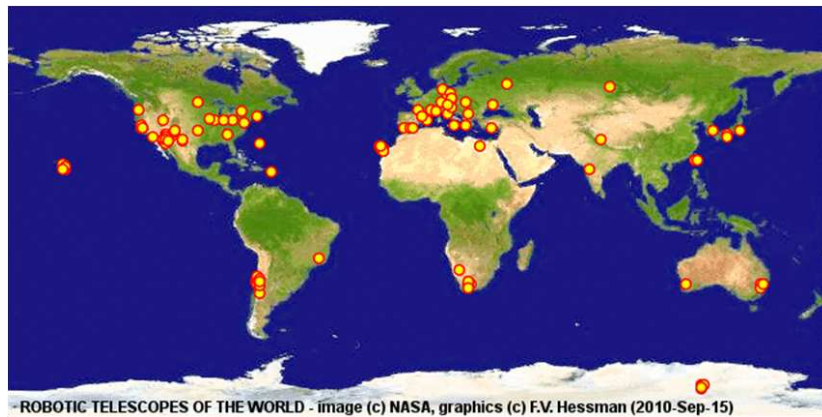


Figure 1. The Robotic Autonomous Observatories worldwide (adopted from Castro Cerón (2011), after Hessman (2001a,b)).

Just for giving to the reader a short panorama about the many small ground- and space-based experiments, not necessarily autonomous, we list the following:

a) **MITSuME (Multicolor Imaging Telescope for Survey and Monstrous Explosions)** has been built to perform Multi-color photometry of NIR /optical afterglow covering the wavebands from K_s to g' allowing the photometric redshift measurements up to $z \sim 10$. Two 50 cm optical telescopes are built at Akeno, Yamanashi in eastern Japan, and at OAO, Okayama in western Japan. Each telescope has a Tricolor Camera, which allows us to take simultaneous images in g' , R_c , and I_c bands. These telescopes respond automatically to GCN alerts and start taking series of tricolor images, which are immediately processed through the analysis pipeline on site. The pipeline consists of source finding, catalog matching, sky coordinates mapping to the image pixels, and photometry of the found sources. An automated search for an optical counterpart is performed. While waiting for GRBs, the MITSuME Telescopes automatically patrol pre-selected interesting objects such as AGNs and galactic transients for multiwavelength studies with Fermi (GLAST) and MAXI (Shimokawabe et al., 2009).

b) **The CHASE (CHilean Automatic Supernova sEarch)** project began in 2007 (Pignata et al., 2009) with the goal to discover young, nearby southern supernovae in order to i) better understand the physics of exploding stars and their progenitors, and ii) refine the methods to derive extra-galactic distances. During the first four years of operation, CHASE has produced more than 130 supernovae, being the most successful project of its type in the southern hemisphere (Hamuy et al., 2012).

c) **PLANET (the Probing Lensing Anomalies NETwork)** is an international collaboration - since 1995 - searching for extrasolar planets via microlensing effects. They work closely with the OGLE, MOA, LCOGT and KMTNet teams forming a global Worldwide consortium, sharing their resources, observations and models real time (Albrow et al., 1995).

d) **RoboNet-II** uses a global network of robotic telescopes to perform follow-up observations of microlensing events in the Galactic Bulge. The current network consists of three 2 m telescopes located in Hawaii and Australia (owned by Las Cumbres Observatory) and the Canary Islands (owned by Liverpool John Moores University). In future years the network will be expanded by deploying clusters of 1 m telescopes in other suitable locations. A principal scientific aim of the RoboNet-II project is the detection of cool extra-solar planets by the method of gravitational microlensing. RoboNet-II acts in coordination with the PLANET microlensing follow-up network and uses an optimization algorithm (web-PLOP) to select the targets and a distributed scheduling paradigm (eS-TAR) to execute the observations. Continuous automated assessment of the observations and anomaly detection is provided by the ARTEMiS system (Tsapras et al., 2009).

e) **LCOGT (the Las Cumbres Observatory Global Telescope Network)** is a research organisation in the process of designing and building a network of robotic telescopes to be used for research in time-domain astrophysics and ed-

ucation. The network will have complete latitude coverage in both hemispheres to allow continuous observations of any target (Hidas et al., 2008).

The LCOGT comprises nine 1-meter and two 2-meter telescopes, all robotic and dynamically scheduled, at five sites spanning the globe (Boroson et al., 2014). This first of LCOGT's 1-m telescopes have been deployed, and the result is a young organization dedicated to time-domain observations at optical and (potentially) near-IR wavelengths. To this end, LCOGT is constructing a world-wide network of telescopes, including the two 2m Faulkes telescopes, as many as 17×1 m telescopes, and as many as 23×40 cm telescopes (Brown et al., 2013).

f) **The eSTAR Project** uses intelligent agent technologies to carry out resource discovery, submit observation requests and analyze the reduced data returned from a meta-network of robotic telescopes (Allan et al., 2004; Allan, Naylor & Saunders, 2006). In 2009 the project lost funding and was shuttered.

g) **OGLE (the Optical Gravitational Lensing Experiment)**, led by Andrzej Udalski of Warsaw University, found the first 3 planets ever detected through microlensing. The international project makes use of the 1.3-meter Warsaw telescope at Las Campanas, Chile, to search for microlensing events. Every night the telescope is pointed toward the same dense field of 100 million stars in the vicinity of the galactic bulge, while the telescope's complex CCD cameras note any change in brightness of any point in the starfield. Every year OGLE detects about 500 microlensing events, but planet detections are extremely rare. As of February 2020, it had found 49 exoplanets.

h) **MOA (Microlensing Observations in Astrophysics)**, led by Yasushi Muraki of Nagoya University, is a Japanese-New Zealand collaboration that uses a 1.8-meter telescope in New Zealand. As of February 2020 it had yielded 24 exoplanets.

i) **KMTNet (the Korea Microlensing Telescope Network)** runs CCD-equipped, 2-meter telescopes at 3 southern observatories. As of February 2020 it had discovered 10 exoplanets.

j) **ROTSE (Robotic Optical Transient Search Experiment)** has developed a next-generation instrument, ROTSE-III, for continuing the search for fast optical transients. The entire system was designed as an economical robotic facility to be installed at remote sites throughout the world (Akerlof et al., 2003).

k) **The (B)urst (O)bserver and (O)ptical (T)ransient (E)xploring (S)ystem (BOOTES)**, a set of instruments that was conceived in 1995 and has contributed significantly to the understanding of astrophysical transients and other high-energy phenomena in the Universe (Castro-Tirado et al., 2012).

l) **The Russian global network of telescopes robot MASTER** (Lipunov et al., 2010). MASTER is very fast positioning alert, follow up and survey twin telescopes Global network with own real-time auto-detection software. MASTER

goal is One Sky in One Night up to 20-21 mag. The network is spread along the whole world. In the following are reported the MASTER Net Sites:

- MASTER-Amur: Russia, near Blagoveschensk. Collaboration with the Blagoveschensk State Pedagogic University. It started in October 2009.
- MASTER-Tunka: Russia, near Irkutsk. Collaboration with the Applied Physics Institute, Irkutsk State University. It started in November 2009.
- MASTER-Ural: Russia, near Ekaterinburg. Collaboration with the Kourouva Astronomical Observatory, Ural State University. It started in December 2008.
- MASTER-Kislovodsk: Russia, Near Kislovodsk, north Caucasus. Kislovodsk Solar Station of the Pulkovo Observatory, and Lomonosov Moscow State University Mountain Observatory (KGO SAI). It started in July 2007.
- MASTER-SAAO: South Africa, Sutherland. Collaboration with the South African Astronomical Observatory (SAAO). It started in December 2014.
- MASTER-IAC: Spain, Canary Islands. Collaboration with the Instituto de Astrofísica de Canarias (IAC). It started in June 2015.
- MASTER-OAFA: Argentina. Collaboration with the Observatorio Astronómico Felix Aguilar (OAFA), Instituto de Ciencias Astronómicas de la Tierra y del Espacio (ICATE), National University of San Juan. It started in February 2012.
- MASTER-Progenitor: Russia, Moscow. Collaboration with the Alexander Krylov Observatory. It started in 2002.
- MASTER-Mexican (MASTER-OAGH - Guillermo Haro Astrophysics Observatory) in Cananea, Sonora, Mexico. Collaboration with the National Institute for Astrophysics, Optics and Electronics (INAOE). It started in December 2021.

m) **Very small satellites for multifrequency astrophysics** have been discussed by Hudec et al. (2017). About the small satellites we can assist to a strong competition (typically for ESA missions, 60 proposals for 1 satellite), and moreover all the system is affected by funding problems.

The development of the Pico (Cube) and Nanosatellites is running at many Universities, mostly with involvement of students for evident goals of education.

The standard size for a CubeSat is 1 Liter Volume, i.e. $10 \times 10 \times 10 \text{ cm}^3$ and typically a weight of $\sim 1.3 \text{ kg}$. Multiple modules are possible, i.e. 3 Units = 3 modules/units, i.e. $10 \times 10 \times 30 \text{ cm}^3$, typically up to 12 Units.

The range of weight of Picosatellites is 0.1-1 kg, Femtosatellites 10-100 g, Nanosatellites 1-10 kg, Microsatellites 10-100 kg.

Recent technological progress allows their use in any field of astrophysics.

Undoubtedly MASTER contributions to transient alerts in Astronomer's telegrams is fundamental. For instance in the period 2013-2014, MASTER contribution is of order 25% of the total as shown in Fig. 2 (after Buckley, 2015).

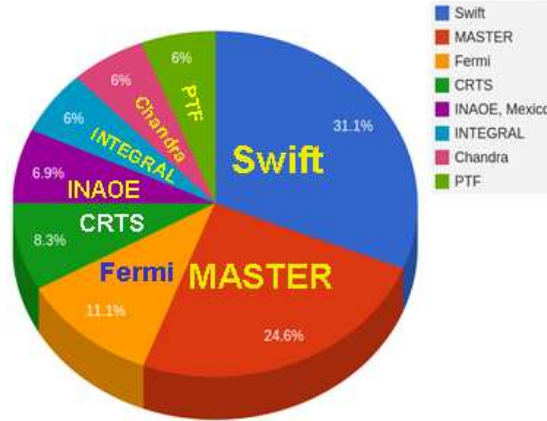


Figure 2. Contribution of different space- and ground-based experiments to the transient alerts in Astronomer's telegrams in the period 2013-2014 (after Buckley, 2015).

Though I have not shown a complete list of small experiments both space- and ground-based, I am able to affirm that small telescopes are unreplaceable tools complementary to larger telescopes and to bigger ground- and space-based multifrequency experiments. In the following section I will present a summary of the selected main results coming from "small" robotic experiments.

3. A summary of the selected results from robotic experiments

The most important news about the many scientific results obtained with the RAOs can be found in the proceedings of the series of Workshops on Robotic Autonomous Observatories (Bloom, Castro-Tirado, Hanlon & Kotani, 2010; Guziy, Pandey, Tello & Castro-Tirado, 2012; Tello, Riva, Hiriart & Castro-Tirado, 2014; Caballero-García, Pandey, Hiriart & Castro-Tirado, 2016a; Caballero-García, Pandey & Castro-Tirado, 2019; Castro-Tirado, Pandey & Caballero-García, 2021).

In the following I will try to report the selected results obtained with the small experiments listed in the previous section, without any pretension to be

exhaustive because the limited space available for this review, and for my limited knowledge.

3.1. MITSuME (Multicolor Imaging Telescope for Survey and Monstrous Explosions)

MITSuME gave a huge amount of information about GRBs. Tens of GNC have been published and can be found for instance looking at the ADS-NASA under the name of Tachibana Yutaro from 2013 to 2019.

Tachibana, Kawai & Pike (2015) presented the long-term light curve data of 3C 454.3 in three energy bands i.e. optical (R-band), X-ray (2-4 keV), and γ -ray (0.1-300 GeV) provided by MITSuME and SMARTS, MAXI/GSC, and Fermi/LAT, and reveal several time variability properties using the optical and the γ -ray flux data. The remarkable result in this research is the finding of a sign of change in the plateau magnitude. The physical parameter of the accretion disk or the relativistic electron in the jet might have changed gradually and significantly.

Fujiwara et al. (2017) report the observations of early GRB afterglows carried out with Akeno 50 cm Telescope from 2008 to 2016. In this period, fourteen GRB afterglows were detected within 1000 seconds after the detections of the prompt emission. They show the optical light curves of the GRB afterglows to discuss timing properties of the external shock. Then, they compare the light curves with the forward/reverse shock models. They discuss the number ratios of the different light-curve types based on the simulation by Gao et al. (2015). Finally, the ratio of magnetic equipartition parameters in the reverse and forward shocks are evaluated as 10-100.

One of the most important results coming from MITSuME was the detection of the outburst on June 15, 2015 after 26 years of quiescence of the black hole binary V404 Cygni (= GS 2023+338). Tachibana et al. (2017) report on the multi-color optical observation (g', RC, and IC) of this object at the beginning of its outburst performed by the MITSuME 50 cm telescope in Akeno, Yamanashi, and the MURIKABUSHI 105 cm telescope at Ishigakijima Astronomical Observatory. The observed SED (Spectral Energy Distribution) from optical to ultraviolet can be expressed by a model consisting of a power-law component and an irradiated disk component.

The long gamma-ray burst GRB 161017A was detected by Fermi and Swift, and its afterglow was observed by the MITSuME 50 cm optical telescope promptly, about 50 s after the burst (Tachibana et al., 2018). They found that the central engine released more energy as jets with a lower photon-emission efficiency in the X-ray flare activity. This qualitative change in the activity may provide us with a hint to understand the mechanisms of jet formation and prompt/X-ray flare emission.

3.2. The CHASE (CHilean Automatic Supernova sEarch)

CHASE is one of the most important hunters of supernovae (SNe). Indeed if we look at the Central Bureau Electronic Telegrams with the name Pignata, P. et al. since 2007 it is possible to see the detection of ~ 188 SNe.

In 2007 the CHilean Automatic Supernova sEarch (CHASE) program started (Pignata et al. 2009) in order to discover young and nearby SNe for which they could directly identify their progenitors in pre-explosion images, or through the fingerprints left by the progenitor in the early phases of evolution of the SN. Intensive spectroscopic and photometric follow-up studies of selected CHASE SNe also allow to test explosion models and learn about the complex physics involved in such phenomena. Last but not least, the CHASE SNe have constituted an important source of targets for the Carnegie Supernova Program (Hamuy et al. 2006) in order to calibrate the SN luminosities and refine methods to determine accurate and precise extragalactic distances. On average CHASE program observes ~ 250 galaxies per night and takes one 80-sec exposures of each galaxy. During the first four years of operation, CHASE has produced more than 130 supernovae, being the most successful project of its type in the southern hemisphere (Hamuy et al., 2012).

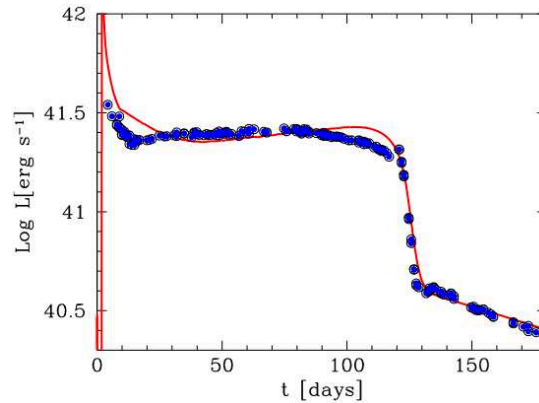


Figure 3. Bolometric light curve of SN 2008bk (blue circles) and hydrodynamic model (red line). The horizontal axis shows the time since explosion (adopted from Hamuy et al., 2012).

Just to show the goodness of CHASE program Fig. 3 shows the bolometric light curve of SN 2008bk in NGC 7793, most likely a low-luminosity SN II-P, which was discovered by Monard (2008) and independently confirmed by CHASE. Hydrodynamic models yield very good fits to CHASE observations, from which it was possible to derive the following parameters: explosion en-

ergy of $E_{\text{exp}} = 0.25 \times 10^{51}$ ergs, progenitor mass $M_{\text{pr}} = 12 M_{\odot}$, initial radius $R_{\text{in}} = 500 R_{\odot}$, and only $0.009 M_{\odot}$ of freshly synthesized radioactive ^{56}Ni . An independent study by Van Dyk et al. (2012) of previously recorded images of the host galaxy taken with the Very Large Telescope and Gemini-South instruments, allowed them to identify the progenitor star and infer a ZAMS mass of $12 M_{\odot}$, in agreement with the hydrodynamic model.

3.3. PLANET (the Probing Lensing Anomalies NETwork)

Gravitational microlensing occurs when a massive compact object (such as a star) passes very near the line-of-sight to a background luminous source (such as another star). The gravitational field of the foreground "lens" bends the light rays from the background "light bulb", resulting in more light reaching the observer's telescope. Significant lensing requires precise source-lens alignment, comparable to the angular radius of the so-called Einstein ring, defined as $\Theta_E = [4GM(1-x)/(c^2D_L)]^{1/2}$, where $x = D_L/D_S$, and M , D_L , and D_S are the lens mass, lens distance, and source star distance, respectively. For typical Galactic microlensing, $\Theta_E \sim 1$ mas, corresponding to separations of 1-5 AU at the position of the lenses. Thus, when these rare precise alignments occur, planetary orbits comparable in size to those of Earth and Jupiter are detectable (Sackett et al., 2003).

Gaudi et al. (2002) analyzed 5 years of PLANET photometry of microlensing events toward the Galactic bulge to search for the short-duration deviations from single-lens light curves that are indicative of the presence of planetary companions to the primary microlenses.

They concluded that less than 33% of M dwarfs in the Galactic bulge have Jupiter-mass companions between 1.5 and 4 AU, and less than 45% have $3M_J$ companions between 1 and 7 AU. These are the first significant limits on planetary companions to M dwarfs.

With generous time allocations at the observatories, PLANET (Probing Lensing Anomalies NETwork) obtained a dense round-the-clock coverage (Albrow et al., 1998) of galactic bulge microlensing events in I with additional observations in R and V with its current network of 1m-class telescopes formed by SAAO 1.0m (South Africa), Danish 1.54m at ESO La Silla (Chile), Canopus 1.0m (Tasmania), and Perth 0.6m (Western Australia), and also with Dutch 0.9m and 2.2m at ESO La Silla, 0.9m and Yale 1.0m at CTIO (Chile), and MSO 50" (Australia). PLANET experiment constrains the abundance and can yield the discovery of planets down to the mass of earth around galactic disk and bulge stars. Data taken until 1999 imply that less than 1/3 of bulge M-dwarfs are surrounded by Jupiter-mass companions at orbital radii between 1 and 4 AU. The current rate of microlensing alerts allows 15-25 Jupiters and 1-3 Earths to be probed per year (Dominik et al., 2004).

Important result has been found by Ranc et al. (2015b) by analysing MOA-2007-BLG-197Lb, the first brown dwarf companion to a Sun-like star detected through gravitational microlensing.

3.4. RoboNet-II

RoboNet-II has developed a complete architecture and supporting software to implement that architecture for the automated detection and characterization of exoplanets detected via the microlensing technique. The RoboNet-1.0 pilot programme in previous seasons has returned promising results and contributed to almost all of the microlensing planetary discoveries to 2009. Current efforts are directed in further automation and restructuring of the scheduling, data acquisition and image processing, improving the alerting system and responses, as well as significant upgrades to the telescope engineering. These involve the deployment of new instruments and electrical safety and performance reliability upgrades. LCOGT is in the process of expanding the robotic network of telescopes. Current plans are for 18 new 1m and 240 .4m telescopes which are expected to be fully integrated and in operation by 2011. The microlensing search for planets, and in particular the method pioneered by the RoboNet project which can potentially make full use of the facilities in an automated way, is a science objective that can be efficiently realized with this network.

3.5. LCOGT (the Las Cumbres Observatory Global Telescope Network)

The LCOGT network V1.0 began full science operations in 2014. It is being used in novel ways to undertake investigations related to supernovae, microlensing events, solar system objects, and exoplanets. The network's user base includes a number of partners, who are providing resources to the collaboration (Borison et al., 2014).

Valenti et al. (2015) presented the first results from the LCOGT Network's Active Galactic Nuclei (AGNs) Key Project, a large program devoted to using the robotic resources of LCOGT to perform time domain studies of active galaxies. They monitored the Seyfert 1 galaxy Arp 151 (Mrk 40) for ~ 200 days with robotic imagers and with the FLOYDS robotic spectrograph at Faulkes Telescope North. Arp 151 was highly variable during this campaign, with V-band light curve variations of ~ 0.3 mag and H_β flux changing by a factor of ~ 3 . They measured robust time lags between the V-band continuum and the H_α , H_β , and H_γ emission lines. The lag for the $\text{He II } \lambda 4686$ emission line is unresolved. They estimated a black hole mass of $M_{\text{BH}} = 6.2_{-1.2}^{+1.4} \times 10^6 M_\odot$.

These results represent the first step to demonstrate the powerful robotic capabilities of LCOGT for long-term AGN time domain campaigns that human intensive programs cannot easily accomplish. Arp 151 is now one of just a few

AGNs where the virial product is known to remain constant against substantial changes in H_β lag and luminosity.

One important result coming from a collaboration among the LCOGT, SMARTS telescopes, HST and XMM-Newton is that about the young (7 Myr) $1.5 M_\odot$ T Tauri star T Cha (Brown et al., 2018). This star shows high variability. The optical extinction varies by at least 3 magnitudes on few hour time-scales. The obscuration is produced by material at the inner edge of the circumstellar disk and therefore characterizing the absorbing material can reveal important clues regarding the transport of gas and dust within such disks. The inner disk of T Cha is particularly interesting, because T Cha has a transitional disk with a large gap at 0.2 – 15 AU in the dust disk and allows study of the gas and dust structure in the terrestrial planet formation zone during this important rapid phase of protoplanetary disk evolution. They examine which spectral features in the different spectral regions (FUV/NUV/optical/X-ray) change and by how much, and thereby determine the location of different emitting regions within the complex stellar/inner disk system relative to the absorbers along the line-of-sight to the stellar photosphere. Understanding these contributions is vital for estimating the properties of the absorbing gas and dust.

Important results are coming from the collaboration among All-Sky Automated Survey for SuperNovae (ASAS-SN, the LCOGT and the TESS, as well as archival data from other missions. Bredall et al.(2020) reported about T Tauri-like "dipper" stars. These stars vary due to transient partial occultation by circumstellar dust, and observations of this phenomenon inform us of conditions in the planet-forming zones close to these stars. They identified 11 dipper stars in the Lupus star forming region. All 11 stars lie above or redward of the zero-age main sequence and have infrared excesses indicating the presence of full circumstellar disks. They obtained reddening-extinction relations for the variability of 7 stars using their combined ASAS-SN-TESS and LCOGT photometry. In all cases the slopes are below the ISM value, suggesting larger grains, and they found a tentative relation between the slope (grain size) and the $Ks - [22 \mu m]$ infrared color regarded as a proxy for disk evolutionary state.

Accretion outbursts are key elements in star formation. ASASSN-13db is a M5-type star with a protoplanetary disk, the lowest-mass star known to experience accretion outbursts. Since its discovery in 2013, it has experienced two outbursts, the second of which started in November 2014 and lasted until February 2017. Sicilia-Aguilar et al. (2017) used high- and low-resolution spectroscopy and time-resolved photometry from the ASAS-SN survey, the LCOGT and the Beacon Observatory to study the light curve of ASASSN-13db and the dynamical and physical properties of the accretion flow. Photometrically and spectroscopically, the 2014-2017 event displays an intermediate behavior between EXors and FUors. The properties of ASASSN-13db suggest that temperatures lower than those for solar-type stars are needed for modeling accretion in very-low-mass systems.

One of the most important contribution of the LCOGT is that of the survey of supernovae (SNe). Indeed, for instance, a multifilter follow-up campaign started on 2015 March 12, when the ASASSN-15ed was already past-maximum, and lasted over two months. It was performed using several telescopes available to the collaboration, including the 1.82-m Copernico Telescope at Mt Ekar (Asiago, Italy), equipped with AFOSC, the LCOGT 1.0-m telescope at McDonald Observatory (Texas, USA) equipped with an SBIG camera, the 10.4-m Gran Telescopio Canarias (GTC) equipped with OSIRIS, the 3.58-m Telescopio Nazionale Galileo (TNG) equipped with DOLORES (LRS), the 2.5-m Nordic Optical Telescope (NOT) with ALFOSC and the 2.0-m Liverpool Telescope (LT) with the IO:O camera, all sited at La Palma (Canary Islands, Spain)(Pastorello et al., 2019).

Another example of the contribution to the knowledge of SNe is the early photometric and spectroscopic observations of SN 2013ej (Valenti et al., 2014), a bright Type IIP supernova (SN) in M 74. SN 2013ej is one of the closest SNe ever discovered. The available archive images and the early discovery help to constrain the nature of its progenitor. The earliest detection of this explosion was on 2013 July 24.125 UT and their spectroscopic monitoring with the FLOYDS spectrographs began on July 27.7 UT, continuing almost daily for two weeks. Daily optical photometric monitoring was achieved with the 1 m telescopes of the LCOGT network, and was complemented by UV data from Swift and near-infrared spectra from Public ESO Spectroscopic Survey of Transient Objects and Infrared Telescope Facility.

Edwards et al. (2021) report photometric follow-up observations of thirteen exoplanets (HATS-1 b, HATS-2 b, HATS-3 b, HAT-P-18 b, HAT-P-27 b, HAT-P-30 b, HAT-P-55 b, KELT-4A b, WASP-25 b, WASP-42 b, WASP-57 b, WASP-61 b and WASP-123 b), as part of the Original Research By Young Twinkle Students (ORBYTS) programme. All these planets are potentially viable targets for atmospheric characterisation and their data, which were taken using the LCOGT network of ground-based telescopes, will be combined with observations from other users of ExoClock^(*) to ensure that the transit times of these planets continue to be well-known, far into the future. These exoplanets will be potential targets for the missions Ariel and JWST that will be able to observe the whole sky, while Twinkle's field of regard is limited to planets within $\pm 40^\circ$ of the ecliptic plane, meaning HAT-P-18 b, HAT-P-55 b and WASP-61 b cannot be studied by this mission.

(*) The ExoClock project, an open, integrated and interactive platform with the purpose of producing a confirmed list of ephemerides for the planets that will be observed by Ariel (Kokori et al., 2021).

3.6. The eSTAR Project

The eSTAR project was a multi-agent system that aimed to implement a heterogeneous network of robotic telescopes for automated observing, and ground-based follow-up to transient events (Allan et al., 2004). By 2007 the eSTAR Project was "live" supporting two real-time observing projects.

One of the most important project was the automated follow-up observations of gamma-ray bursts (GRBs) performed using the 3.8 m United Kingdom Infrared Telescope (UKIRT) operated by Joint Astronomy Centre in Hawaii (JACH). The first ground based observations of GRB 090423 were triggered via the eSTAR Project, with initial observations by the Swift GRB Mission automatically followed by UKIRT just a few minutes after the initial observation by the SWIFT satellite. The observations autonomously triggered by the eSTAR software were reported in Tanvir et al. (2009). This GRB was, at the time of discovery, the most distant object then known in the Universe. GRB090423 lies at a redshift of $z \sim 8.2$, implying that massive stars were being produced and dying as GRBs ~ 630 Myr after the Big Bang. The burst also pinpoints the location of its host galaxy.

Another important program was the search for extra-solar planets by placing observations on the RoboNet system of telescopes on behalf of the PLANET collaboration. The technique of gravitational microlensing is used to monitor large numbers of stars in the galactic bulge looking for the tell-tale signature of cool planets orbiting those stars. The project also operated the heaviest used of the initial generation of Virtual Observatory VOEvent brokers, exposing its real-time alert system to other collaborators, like the TALONS (White et al., 2004).

Unfortunately in 2009 the project lost funding and was shuttered.

3.7. OGLE (the Optical Gravitational Lensing Experiment)

The OGLE collaboration, together with others span in detecting exoplanets from brown dwarfs to Earth and super-Earth-mass planets, to sub-Saturn-mass planets, to Jupiter and super-Jupiter-mass planets, to neutron stars and low mass black holes.

Skowron et al. (2015) reported the discovery of a Jupiter-mass planet orbiting an M-dwarf star that gave rise to the microlensing event OGLE-2011-BLG-0265. Such a system is very rare among known planetary systems and thus the discovery is important for theoretical studies of planetary formation and evolution. High-cadence temporal coverage of the planetary signal, combined with extended observations throughout the event, allows them to accurately model the observed light curve. However, the final microlensing solution remains degenerate, yielding two possible configurations of the planet and the host star. In the case of the preferred solution, the mass of the planet is $M_{\text{planet}} = 0.9 \pm 0.3 M_{\text{J}}$, and the planet is orbiting a star with a mass $M = 0.22 \pm 0.06 M_{\odot}$. The

second possible configuration (2σ away) consists of a planet with $M_{\text{planet}} = 0.6 \pm 0.3 M_{\text{J}}$ and host star with $M = 0.14 \pm 0.06 M_{\odot}$. The system is located in the Galactic disk 3-4 kpc toward the Galactic bulge. In both cases, with an orbit size of 1.5-2.0 AU, the planet is a "cold Jupiter" – located well beyond the "snow line" of the host star.

Bond et al. (2017) reported the discovery of the lowest mass ratio exoplanet to be found by the microlensing method in the light curve of the event OGLE 2016-BLG-1195. This planet revealed itself as a small deviation from a microlensing single lens profile from an examination of the survey data. The duration of the planetary signal is ~ 2.5 h. The measured ratio of the planet mass to its host star is $q = (4.2 \pm 0.7) \times 10^{-5}$. They further estimate that the lens system is likely to comprise a cold ~ 3 Earth mass planet in an ~ 2 AU wide orbit around a 0.2 Solar mass star at an overall distance of 7.1 kpc.

The discovery and analysis of a Saturn-mass planet in the microlensing event OGLE-2017-BLG-0406, which was observed both from the ground and by the Spitzer satellite in a solar orbit have been reported by Hirao et al. (2020). At high magnification, the anomaly in the light curve was densely observed by ground-based-survey and follow-up groups, and it was found to be explained by a planetary lens with a planet/host mass ratio of $q = 7.0 \times 10^{-4}$ from the light-curve modeling. The ground-only and Spitzer-"only" data each provide very strong one-dimensional (1D) constraints on the 2D microlens parallax vector π_{E} . When combined, these yield a precise measurement of π_{E} and of the masses of the host $M_{\text{host}} = 0.56 \pm 0.07 M_{\odot}$ and planet $M_{\text{planet}} = 0.41 \pm 0.05 M_{\text{J}}$. The system lies at a distance $D_{\text{L}} = 5.2 \pm 0.5$ kpc from the Sun toward the Galactic bulge, and the host is more likely to be a disk population star according to the kinematics of the lens. The projected separation of the planet from the host is $a_{\perp} = 3.5 \pm 0.3$ AU (i.e., just over twice the snow line).

Zang et al. (2020) reported the discovery and analysis of a sub-Saturn-mass planet in the microlensing event OGLE-2018-BLG-0799. The planetary signal was observed by several ground-based telescopes, and the planet-host mass ratio is $q = (2.65 \pm 0.16) \times 10^{-3}$. The ground-based observations yield a constraint on the angular Einstein radius Θ_{E} , and the microlens parallax π_{E} is measured from the joint analysis of the Spitzer and ground-based observations, which suggests that the host star is most likely to be a very low-mass dwarf. A full Bayesian analysis using a Galactic model indicates that the planetary system is composed of an $M_{\text{planet}} = 0.22^{+0.19}_{-0.06} M_{\text{J}}$ planet orbiting an $M_{\text{host}} = 0.080^{+0.080}_{-0.020} M_{\odot}$, at a distance of $D_{\text{L}} = 4.42^{+1.73}_{-1.23}$ kpc. The projected planet-host separation is $r_{\perp} = 1.27^{+0.45}_{-0.29}$ AU, implying that the planet is located beyond the snow line of the host star. However, because of systematics in the Spitzer photometry, there is ambiguity in the parallax measurement, so the system could be more massive and farther away.

Zang et al. (2021a) report the discovery of KMT-2020-BLG-0414Lb, with a planet-to-host mass ratio = $3\text{-}4 M_{\oplus}$ at 1σ , which is the lowest mass-ratio mi-

cro lensing planet to date. The detection of this planet, despite the considerable difficulties imposed by COVID-19 (two KMT sites and OGLE were shut down), illustrates the potential utility of this program.

With a mass ratio of $q \sim 1.27 \pm 0.07$ or $\sim 1.45 \pm 0.15 \times 10^{-5}$, OGLE-2019-BLG-0960Lb is the smallest mass-ratio microlensing planet ever found (Yee et al., 2021). The annual parallax effect combined with the finite source effect indicate the host star is an M-dwarf at $D_L \leq 1$ kpc with a super-Earth planet orbiting between 1 and 2 AU. Indeed, the mass of the host star ($M_L = 0.3 - 0.6 M_\odot$), the mass of its planet ($m_p = 1.4-3.1 M_\oplus$), the projected separation between the host and planet ($a_\perp = 1.2-2.3$ AU), and the distance to the lens system ($D_L = 0.6-1.2$ kpc).

By using measurements with OGLE, MOA, HST, and Gaia, Lam et al. (2022) presented the analysis of five black hole (BH) candidates identified from gravitational microlensing surveys. One of the five targets (OGLE-2011-BLG-0462/MOA-2011-BLG-191 or OB110462 for short) is the first definitive discovery of a compact object through astrometric microlensing and it is most likely either a neutron star or a low-mass black hole (its mass ranging from 1.6 to 4.2 M_\odot). This compact object lens is relatively nearby (690-1370 pc) and has a slow transverse motion of < 25 km/s. For the remaining four candidates, the lens masses are $< 2 M_\odot$ and they are unlikely to be black holes; but two of the four are likely white dwarfs or neutron stars.

Another important result is that reported by Shin et al. (2022). OGLE-2016-BLG-1093 is a planetary microlensing event that is part of the statistical Spitzer microlens parallax sample. The precise measurement of the microlens parallax effect for this event, combined with the measurement of finite source effects, leads to a direct measurement of the lens masses and system distance: $M_{\text{host}} = 0.38-0.57 M_\odot$, $m_p = 0.59-0.87 M_J$, and the system is located at the Galactic bulge ($D_L \sim 8.1$ kpc).

The transition objects between stars and planets are very probably brown dwarfs. But this transition is poorly understood. Mass measurements are generally difficult for isolated objects but also for brown dwarfs orbiting low-mass stars, which are often too faint for spectroscopic follow-up. Herald et al. (2022) analyse the microlensing event OGLE-2019-BLG-0033/MOA-2019-BLG-035, which is due to a binary system composed of a brown dwarf orbiting a red dwarf. The result obtained – thanks to Spitzer and extensive ground observations – is an accurate estimates of all microlensing parameters, including parallax, source radius and orbital motion of the binary lens. After accurate modeling, they find that the lens is composed of a red dwarf with mass $M_1 = 0.149 \pm 0.010 M_\odot$ and a brown dwarf with mass $M_2 = 0.0463 \pm 0.0031 M_\odot$, at a projected separation of $a_\perp = 0.585$ AU. The system has a peculiar velocity that is typical of old metal-poor populations in the thick disk.

3.8. MOA (Microlensing Observations in Astrophysics)

In a collaboration between MOA and OGLE, Hirao et al. (2017) reported the discovery and the analysis of the planetary microlensing event, OGLE-2013-BLG-1761. The lens system is located $D_L = 6.9_{-1.2}^{+1.0}$ kpc away from us and the host star is an M/K dwarf with a mass of $M_L = 0.33_{-0.19}^{+0.32} M_\odot$ orbited by a super-Jupiter mass planet with a mass of $m_P = 2.7_{-1.5}^{+2.5} M_J$ at the projected separation of $a_\perp = 1.8_{-0.5}^{+0.5}$ AU.

Blackman et al. (2021) reported the non-detection of a main-sequence lens star in the microlensing event MOA-2010-BLG-477Lb12 using near-infrared observations from the Keck Observatory. They determined that this system contains a $0.53 \pm 0.11 M_\odot$ white-dwarf host orbited by a 1.4 ± 0.3 Jupiter-mass planet with a separation on the plane of the sky of 2.8 ± 0.5 AU, which implies a semi-major axis larger than this. This system is evidence that planets around white dwarfs can survive the giant and asymptotic giant phases of their host's evolution, and supports the prediction that more than half of white dwarfs have Jovian planetary companions (Schreiber et al., 2019). Located at approximately 2.0 kpc towards the centre of our Galaxy, it is likely to represent an analogue to the end stages of the Sun and Jupiter in our own Solar System.

As part of a systematic modelling effort in the context of a > 10 -yr retrospective analysis of MOA's survey observations to build an extended MOA statistical sample, Ranc et al. (2021) analysed the light curve of the planetary microlensing event MOA-2014-BLG-472. This event provides weak constraints on the physical parameters of the lens, as a result of a planetary anomaly occurring at low magnification in the light curve. They used a Bayesian analysis to estimate the properties of the planet, based on a refined Galactic model and the assumption that all Milky Way's stars have an equal planet-hosting probability. They found that a lens consisting of a $1.9_{-1.2}^{+2.2} M_J$ giant planet orbiting a $0.31_{-0.19}^{+0.36} M_\odot$ host at a projected separation of 0.75 ± 0.24 AU is consistent with the observations and is most likely, based on the Galactic priors. The lens most probably lies in the Galactic bulge, at $7.2_{-1.7}^{+0.6}$ kpc from Earth.

3.9. KMTNet (the Korea Microlensing Telescope Network)

Jung et al. (2020a) reported the discovery of a planet in the microlensing event OGLE-2018-BLG-1269 with a planet-host mass ratio $q \sim 6 \times 10^{-4}$, i.e., 0.6 times smaller than the Jupiter/Sun mass ratio. Combined with the Gaia parallax and proper motion, a strong one-dimensional constraint on the microlens parallax vector allows them to significantly reduce the uncertainties of lens physical parameters. A Bayesian analysis that ignores any information about light from the host yields that the planet is a cold giant ($M_2 = 0.69_{-0.22}^{+0.44} M_J$) orbiting a Sun-like star ($M_1 = 1.13_{-0.35}^{+0.72} M_\odot$) at a distance of $D_L = 2.56_{-0.62}^{+0.92}$ kpc. The projected planet-host separation is $a_\perp = 4.61_{-1.17}^{+1.70}$ AU.

Jung et al. (2020b) – with large collaboration among KMTNet, OGLE, and MOA – found that KMT-2019-BLG-0842Lb is a cold planet located beyond the snow line of its host, and the planet/host mass ratio is $q = (4.09 \pm 0.27) \times 10^{-5}$, which is similar to the ratio of Uranus/Sun in the solar system. The discovery of the planetary system, together with similar systems previously discovered, provides evidence that such planets are not rare. Nevertheless, further discoveries will be necessary to estimate the frequency and characterize the distribution of such planets.

In order to exhume the buried signatures of "missing planetary caustics" in Korea Microlensing Telescope Network (KMTNet) data, Zang et al. (2021b) conducted a systematic anomaly search of the residuals from point-source point-lens fits, based on a modified version of the KMTNet EventFinder algorithm. This search revealed the lowest-mass-ratio planetary caustic to date in the microlensing event OGLE-2019-BLG-1053, for which the planetary signal had not been noticed before. The planetary system has a planet-host mass ratio of $q = (1.25 \pm 0.13) \times 10^{-5}$. A Bayesian analysis yielded estimates of the mass of the host star, $M_{\text{host}} = 0.61_{-0.24}^{+0.29} M_{\odot}$, the mass of its planet, $M_{\text{planet}} = 2.48_{-0.98}^{+1.19} M_{\oplus}$, the projected planet-host separation, $a_{\perp} = 3.4_{-0.5}^{+0.5}$ AU, and the lens distance, $D_L = 6.8_{-0.9}^{+0.6}$ kpc. The discovery of this very-low-mass-ratio planet illustrates the utility of their method and opens a new window for a large and homogeneous sample to study the microlensing planet-host mass ratio function down to $q \sim 10^{-5}$.

3.10. ROTSE (Robotic Optical Transient Search Experiment)

Following the results from ROTSE-I instrument described by Woźniak et al. (2004) it is possible to understand the importance of such instrument. They presented the Northern Sky Variability Survey (NSVS), the most extensive temporal record of the sky on large spatial scales, updated to 2004. All of the survey data is available to the astronomical community and can be searched efficiently using the public SkyDOT database. The database contains a total of 3.35 billion measurements for approximately 14 million objects in the 8-15.5 mag range. Time sampling over 1 full year is between twice per night and once every four nights, on average. The ROTSE-I instrument has achieved a complete spatial coverage of the northern hemisphere and a large fraction of the southern sky using remarkably low cost hardware. These two factors pose limits to the level of detail at which variability of the sky was recorded: low spatial resolution, spatial sensitivity variations, a nonstandard filter, and complicated systematics near the Galactic plane. Despite its limitations, the NSVS is a truly rich source of information on stellar variability. Among stars in the Galaxy, the fraction of variables with amplitudes detectable by the NSVS is about $\sim 1\%$ (Eyer, 1999; Eyer & Cuipers 2000). Based on that and on preliminary results in Akерlof et al. (2000), one can expect that tens of thousands of new variable stars with good uniform quality light curves are present in the data set. Current

database schema needs to be expanded along the lines described in Woźniak et al. (2002) to accommodate various types of variables and provide classification capability. The NSVS combined with astrometric catalogs providing distances and motions, as well as multicolor surveys (2MASS, or even SDSS in a narrow magnitude range) will enable a comprehensive look at the Galaxy as traced by variable stars. The NSVS objects are bright and therefore the preferred targets for detailed spectroscopic and astrometric work. The spatial resolution of the survey is not far from that of high-energy sky catalogs like the ROSAT All Sky Survey (Voges et al., 1999) or the XMM Catalog of Serendipitous Sources (Watson, 2003), and therefore it is well suited for cross-correlations. Perhaps the most exciting questions to be attacked using the NSVS are regarding rare, hard to find objects. The astronomical literature provides numerous unexplained reports of variability events on normal stars (e.g., Schaefer, King, & Deliyannis 2000 and references therein). Photometric monitoring data for active galactic nuclei (AGNs) providing diagnostics of accretion flows is valuable, but limited. Only a few bright AGNs are within the magnitude limit of the NSVS, so the real contribution to AGN physics will require deeper flux limits and better resolution in future projects. A major but low cost improvement in data usability would be the use of a set of standard filters before starting deeper surveys with more frequent time sampling. Small robotic telescopes with automated data-processing pipelines are the best candidates for closing the gap in the current level of temporal monitoring of the sky. The computing power to perform on-line photometry is available. Experiments like RAPTOR (Vestrand et al., 2002) are starting to tackle the problem of real-time detection and immediate follow-up of short timescale phenomena. One can envision a monitoring system capable of partial interpretation of various events occurring on a variety of timescales and notifying subscribers about interesting changes of objects in their scientific problem domain. The main challenge is making the immense data stream comprehensible by putting enough smarts into the software. The sky itself is the ultimate astronomical database that should be mined continuously and in real time.

ROTSE-II was a set of twin 0.45 m aperture, f/1.9 telescopes to be operated in stereo mode. The optical design was performed by Mel Kreitzer (1976) and Jacob Moskovich (1978) at OPCON Associates, Inc. Each telescope covers a field of view of $1.9^\circ \times 1.9^\circ$ and was expected to achieve a limiting magnitude of $m_v \simeq 18$ for a 10-second exposure. By scanning around the most probable burst location, a $16^\circ \times 16^\circ$ error box can be searched in 16 minutes. More accurate initial coordinates will permit faster scans or deeper images (Marshall et al., 1997). By co-adding frames, both ROTSE-I and ROTSE-II was to be able to detect objects considerably fainter than the limits quoted above. In particular, ROTSE-II was be able to find optical transients at the levels discovered for GRB 970228 and GRB 970508.

The observation of a prompt optical flash from GRB 990123 convincingly demonstrated the value of autonomous robotic telescope systems. Pursuing a

program of rapid follow-up observations of GRBs. For this reason ROTSE developed a next-generation instrument, ROTSE-III, that continues the search for fast optical transients. The entire system was designed as an economical robotic facility to be installed at remote sites throughout the world. There are seven major system components: optics, optical tube assembly, CCD camera, telescope mount, enclosure, environmental sensing and protection, and data acquisition. Each is described in turn in the hope that the techniques developed will be useful in similar contexts elsewhere (Akerlof et al., 2003). ROTSE-III is a homogeneous worldwide array of 4 robotic telescopes. They were designed to provide optical observations of GRB afterglows as close as possible to the start of γ -ray emission. ROTSE-III is fulfilling its potential for GRB science, and provides optical observations for a variety of astrophysical sources in the interim between GRB events (Yost et al., 2006).

Ruiz-Velasco et al. (2007) report on follow-up observations of the GRB 060927 using the robotic ROTSE-IIIa telescope and a suite of larger aperture ground-based telescopes. They discuss the implications of this work for the use of GRBs as probes of the end of the dark ages and draw three main conclusions: (1) GRB afterglows originating from $z > 6$ should be relatively easy to detect from the ground, but rapid near-infrared monitoring is necessary to ensure that they are found; (2) the presence of large H_I column densities in some GRB host galaxies at $z > 5$ makes the use of GRBs to probe the reionization epoch via spectroscopy of the red damping wing challenging; and (3) GRBs appear crucial to locate typical star-forming galaxies at $z > 5$, and therefore the type of galaxies responsible for the reionization of the universe.

Quinby et al. (2012) presented a sample of 23 spectroscopically confirmed Type Ia supernovae (SNe Ia) that were discovered in the background of galaxy clusters targeted by ROTSE-IIIb and use up to 18 of these to determine the local ($\bar{z} = 0.05$) volumetric rate. They found that the total SNe Ia rate may be higher than the canonical value.

One more interesting result coming from ROTSE-III is relative to the Luminosity Function (LF) of GRBs. Indeed, Cui et al. (2014) estimated, from a uniform sample of 58 GRBs from observations with the ROTSE-III, the cumulative distribution of optical emission at 100 s, well described by an exponential rise and power-law decay, a broken power law, and Schechter LFs^(*). A single power-law (SPL) LF, on the other hand, is ruled out with high confidence.

(*) The Schechter luminosity function provides a parametric description of the space density of galaxies as a function of their luminosity.

3.11. The (B)urst (O)bserver and (O)ptical (T)ransient (E)xploring (S)ystem (BOOTES)

The Burst Observer and Optical Transient Exploring System (BOOTES) was considered as a part of the preparations for ESA's INTEGRAL satellite, and

was developed in Spain, as a Spanish-Czech collaboration, devoted to study optical emissions from GRBs. It makes use of two sets of wide-field cameras, 240 km apart, and two robotic 0.3-m telescopes. The first observing station (BOOTES-1) was located at the Estación de Sondeos Atmosféricos in Centro de Experimentación de El Arenosillo, a dark-sky site near Mazagón (Huelva), center owned by the Instituto Nacional de Técnica Aeroespacial (INTA).

The first light was obtained in July 1998. During the test phase, it has provided rapid follow-up observations with the wide-field cameras for 19 GRBs detected by BATSE aboard CGRO, and narrow-field imaging for 6 bursts. Limiting magnitudes for any GRB optical afterglow are $I \sim 13$ and $R \sim 16.5$, a few minutes after the events (Castro-Tirado et al., 1999, 2000).

The second observing station was opened in 2001 and it was located at the Estación Experimental de La Mayora (dubbed BOOTES-2), 240 km apart. The latter is run by the Consejo Superior de Investigaciones Científicas (CSIC). BOOTES-2 has been equipped with COLORES (Compact Low Resolution Spectrograph) (Rabaza et al., 2013). It is a spectrograph designed to be lightweight enough to be carried by the high-speed robotic telescope 60 cm (BOOTES-2). It works in the wavelength range of (3800 - 11500) Å and has a spectral resolution of (15 - 60) Å. The primary scientific target of the spectrograph is a prompt GRB follow-up, particularly the estimation of redshift.

In 2009 BOOTES started to expand abroad, adding stations BOOTES-3 in Lauder (South Island, New Zealand), BOOTES-4 (2011, Lijiang Astronomical Observatory in Yunnan, China, Guziy et al., 2013), BOOTES-5 (2013, San Pedro Martir, Mexico), BOOTES-6 (2021, Boyden Observatory, South Africa) and eventually finishing the world-wide coverage by BOOTES-7 (2023, San Pedro de Atacama, Chile).

Since the first light on 1998, more than a hundred of GRBs have been observed with BOOTES, some of them only ≈ 30 s after the onset of the γ -ray event. More in general BOOTES has been used for the follow-up of optical transient, such as the X-ray/Be system A0535+26/HDE245770 and the accreting black hole SS 433 (e.g. Caballero-García et al., 2014). Interesting results from BOOTES-2 and COLORES are those of the DG Canum Venaticorum (DG CVn). This is a very fast rotating star and this fact has been associated to the youth of the star: 30 Myr (Caballero-García et al., 2016b and the references therein). This star experienced a big flare that can be explained by the presence of (a) large active region(s) on the surface of the star. Such activity is similar to the most extreme solar flaring events. This points towards a plausible extrapolation between the behaviour from the most active red-dwarf stars and the processes occurring in the Sun (Caballero-García et al., 2015).

A contribution of BOOTES-2/COLORES has been given during the sub-second optical flaring in V404 Cyg during the 2015 outburst peak (Gandhi et al., 2016). Indeed, the most prominent optical emission line in the case of V404 Cyg is H_{α} , which falls in the r' band. They estimated the relative flux contribution of H_{α} , being the emission line strength relative to continuum strongly variable.

One of the most significant result of this investigation is the following: under the compact jet scenario, it is possible to place limits on the magnetic field strength at the synchrotron emission zone of $B \leq 2 \times 10^5$ G, and a zone size $R \geq 140 R_G$. If the fastest flares arise within this zone, the variability time-scale of the unresolved flares of < 24 ms implies $R \leq 500 R_G$, being R_G the gravitational radius.

An important contribution of BOOTES to the knowledge of GRBs is coming from ~ 70 GNC (GRB Coordinates Network, Circular Service) publications where optical observations of different GRBs have been reported. They can be found in the NASA-ADS under the name Caballero-Garcia, M.D. from 2016 to 2022 (March 17th).

3.12. The Russian global network of telescopes robot MASTER

The Russian global network of telescopes robot MASTER has the fundamental advantage that the observations are performed with identical telescopes equipped with identical photometers. No other network of telescopes can boast such a feature.

I will discuss in the following some of the numerous important results obtained with the MASTER Robotic Net.

On 2015 June 15, the Swift space observatory discovered that the Galactic black hole candidate V 404 Cyg was undergoing another active X-ray phase, after 25 years of inactivity. The 12 telescopes of the MASTER Global Robotic Net located at six sites across four continents were the first ground-based observatories to start optical monitoring of the microquasar after its gamma-ray wake up at 18h 34m 09s U.T. on 2015 June 15 (Lipunov et al., 2016a). The discovery of variable optical linear polarization, changing by 4%-6% over a timescale of ~ 1 hr, on two different epochs, allows to conclude that the additional variable polarization arises from the relativistic jet generated by the black hole in V 404 Cyg. The polarization variability correlates with optical brightness changes, increasing when the flux decreases. The relativistic jet generated by the black hole was only observed until 2015 June 15 in nonthermal radio and hard X-ray emission.

Gorbovskey et al. (2016) reported early optical linear polarization observations of two GRBs made with the MASTER Robotic Net. They found the minimum polarization for GRB 150301B to be 8% at the beginning of the initial stage, whereas they detected no polarization for GRB 150413A either at the rising branch or after the burst reached the power-law afterglow stage. This is the earliest measurement of the polarization (in cosmological rest frame) of GRBs. By the way, they reported the discovery of the optical counterpart of one of the two bursts: GRB 150413A. This GRB was detected by BAT instrument of Swift observatory (Markwardt et al. 2015), and soon after was associated to an optical transient by the telescope of MASTER Robotic Net located at Tunka astrophysical centre near Baikal lake.

Important contribution of the MASTER Robotic Net was the early discovery of the optical afterglow of the GRB 140801A in the 137 deg^2 3σ error-box of the Fermi Gamma-ray Burst Monitor (GBM) (Lipunov et al., 2016b). Indeed, MASTER is the only observatory that automatically reacts to all Fermi alerts. GRB 140801A is one of the few GRBs whose optical counterpart was discovered solely from its GBM localization. The optical afterglow of GRB 140801A was found by MASTER Global Robotic Net 53 s after receiving the alert, making it the fastest optical detection of a GRB from a GBM error-box. Spectroscopy obtained with the 10.4-m Gran Telescopio Canarias and the 6-m Big Telescope Alt-azimuth of the Special Astrophysical Observatory of the Russian Academy of Sciences reveals a redshift $z = 1.32$. The rest-frame bolometric isotropic energy release and peak energy of the burst are $E_{\text{iso}} = 5.54_{-0.24}^{+0.26} \times 10^{52}$ erg and $E_{\text{p,rest}} \simeq 280$ keV, respectively, which is consistent with Amati's relation.

Lipunov et al. (2017a) presented the discovery of the rare explosive star MASTER OTJ004207.99+405501.1 – a luminous red nova (LRN) – in the Andromeda galaxy M31 N2015-01a, and long-term observations of its light curve with the MASTER network of robotic telescopes. Monitoring has been carried out for 72 d after the discovery of this LRN. They found that the multicolour passband light curves of the LRN are consistent with an initial common envelope radius of $10 R_{\odot}$, a merger mass of $3 M_{\odot}$ and an explosion energy of 3×10^{48} erg. As a result, the phenomenon of novae consists of two classes: classical nuclear novae and more rare events (red novae) connected with the loss of compact common envelopes.

One of the most important results obtained with the Global MASTER Robotic Net has been reported by Lipunov et al. (2017b). They received the GW 150914 alert message with the error region just over a day after the GW-event, on 2015 September 16. All telescopes in the MASTER network began observing different parts of the GW 150914 error region when the corresponding areas became visible. The first images in response to the GW 150914 alert were taken at the MASTER-SAAO observatory at 2015 September 16 20:18:11 UT, and the follow-up was extended until September 22. The results obtained with this campaign of observations are consistent with the conclusion that GWs from GW 150914 were produced in a binary black hole merger. The detection of this event was predicted in 1997 on the basis of the Scenario Machine population synthesis calculations, as discussed in Lipunov et al. (2017c and in the references therein).

During this campaign of observations eight optical transient (OTs) were detected. Among them there are: (1) MASTER OT J040938.68-541316.9 (a possible SN discovery); (2) MASTER OT J070747.72-672205.6 (a possible U Gem type (dwarf nova outburst) detection); (3) MASTER OT J042822.91-604158.3 discovery (possible dwarf nova outburst). The data cannot exclude that MASTER OT J040938.68-541316.9 exploded on 2015 September 14.

On 2017 August 17 the merger of two compact objects with masses consistent with two neutron stars was discovered through gravitational-wave (GW170817),

γ -ray (GRB 170817A), and optical (SSS17a/AT2017gfo) observations. The optical source was associated with the early-type galaxy NGC 4993 at a distance of just ~ 40 Mpc, consistent with the gravitational-wave measurement, and the merger was localized to be at a projected distance of ~ 2 kpc away from the galaxy's center (Abbott et al., 2017a,b).

Lipunov et al. (1995) predicted the NS-NS merger at a distance of ≤ 50 Mpc and the possibility of detecting GWs!

This prediction was born by the "Scenario Machine" that describes the evolution of gravimagnetic rotators (Lipunov, 1987; Lipunov, & Postnov, 1988), and commented by Giovannelli (2016).

The MASTER Global Robotic Net telescopes obtained the first image of the NGC 4993 host galaxy. An optical transient, MASTER OTJ130948.10-232253.3/SSS17a was later found, which appears to be a kilonova resulting from the merger of two neutron stars (NSs) (Lipunov et al., 2017d). They described this independent detection and photometry of the kilonova made in white light, and in B, V, and R filters. They noted that the luminosity of this kilonova in NGC 4993 is very close to those measured for other kilonovae possibly associated with GRB 130603 and GRB 080503. The agreement between the observed absolute magnitudes and characteristic luminosities evoke the old idea about viewing GRBs as standard candles (Lipunov, Postnov & Prokhorov, 2001). However, we are now dealing with kilonovae that accompany short GRB events. Here there is rather an analogy with Type Ia SNe. Both kinds of event may represent collisions of compact stars: binary white dwarfs and binary NSs in the case of supernovae and kilonovae, respectively.

GRB 161017A was first detected at γ -ray wavelengths by the Lomonosov and Swift instruments. Following the Swift's transmission of a GCN alert, the MASTER robotic telescopes were automatically directed to the preliminary GRB source coordinates to begin their optical observations (Sadovnichy et al., 2018). Following the MASTER automatic observation, the analysis software reported the detection of a GRB optical emission and signaled the world's largest optical telescope, the 10.4 m Gran Telescopio Canarias (GTC) located in the Canary Islands, which recorded the burst and from the redshift value determined the host galaxy to be about 10 billion light years away.

Its γ -ray emission measured up to 0.5 MeV. At a redshift $z = 2.0127$, the most recent findings are $H_0 = 67.3 \text{ km s}^{-1} \text{ Mpc}^{-1}$, $\Omega_\Lambda = 0.685$, $\Omega_M = 0.315$ (Planck Collaboration et al., 2016), $E_{\text{iso}} \simeq 10^{53} \text{ erg}$ (for a GRB fluence of $3 \times 10^{-6} \text{ erg s}^{-1}$ and a luminosity distance of $D_L = 16.081 \text{ Gpc}$). There is no apparent forward shock emission in the optical light curve, and only an afterglow emission component is visible, peaking at around 100 s. If we interpret these observations according to the correlation provided by Liang et al. (2010), it is possible to infer the initial Lorentz factor to be $\Gamma_0 \sim 300$.

MASTER Robotic Net is useful also for the study of SNe. Indeed, for example, MASTER OT J120451.50+265946.6 (M 12045), discovered by the MASTER Global Robotic Net, is a Type Ib supernova (SN) that exploded in NGC

4080. Singh et al. (2019) presented the BVRI photometric and spectroscopic observations up to ~ 250 days since B_{\max} . At the time of discovery the SN was a few weeks past maximum light and their observations capture the linearly declining light curve phase. M 12045 declined faster as compared to SNe 1999dn and 2009jf at comparable epochs. Rigorous spectroscopic monitoring revealed that M 12045 is a normal Type Ib SN. The analysis of the nebular phase spectra indicated that $\sim 0.90 M_{\odot}$ of O is ejected in the explosion. The line ratio of $[O\text{I}]$ and $[\text{CaII}]$ in the nebular phase supports a massive WR progenitor with main sequence mass of $\sim 20 M_{\odot}$.

Important efforts have been performed in searching for the High-Energy (HE) neutrino progenitor. Lipunov et al. (2020) presented the earliest astronomical observation of a HE neutrino error box of which the variability was discovered after HE-neutrino detection. The one robotic telescope of the MASTER global international networks automatically imaged the error box of the very HE-neutrino event IceCube-170922A. Observations were carried out in minutes after the detection of the IceCube-170922A neutrino event, obtained by the IceCube observatory at the South Pole. MASTER found the blazar TXS 0506+056 to be in the off-state after one minute and then switched to the on-state no later than two hours after the event. The effect is observed at a 50σ significance level.

The event that they discovered, namely the decrease of the brightness of the TXS 0506+056 blazar near the neutrino detection time, provides complementary and very compelling evidence for the link between the blazar and the IceCube-170922 neutrino event. They analyzed also archival data (MASTER unique 518 photometry data for 16 yr), which they found to be consistent with this fact. They also proposed a hypothesis explaining the anticorrelation of the optical and neutrino flux. An increase in neutrino flux means that up to half of the protons disappear. If one assumes that these protons produce synchrotron optical radiation, then any increase in neutrino luminosity will lead to a decrease in the optical brightness of the blazar.

Interesting results are coming from polarimetric measurements obtained with the RINGO3 (Słowikowska et al., 2016) and MASTER II (Lipunov et al., 2010) polarimeters on GRB 190114C (Jordana-Mitjans et al., 2020). They report multicolor optical imaging and polarimetry observations of the afterglow of the first TeV-detected GRB, GRB 190114C. Observations began 31 s after the onset of the GRB and continue until ~ 7000 s postburst. The unexpectedly low intrinsic polarization degree in GRB 190114C can be explained if largescale jet magnetic fields are distorted on timescales prior to reverse shock emission.

Buckley et al. (2021) reported on results of spectropolarimetry of the afterglow of the long GRB 191221B, obtained with SALT/RSS and VLT/FORS2, as well as photometry from two telescopes in the MASTER Global Robotic Net, at the MASTER-SAAO (South Africa) and MASTER-OAFA (Argentina) stations. Prompt optical emission was detected by MASTER-SAAO 38 s after the alert, which dimmed from a magnitude (white-light) of ~ 10 to 16.2 mag over a period of ~ 10 ks, followed by a plateau phase lasting ~ 10 ks and then a decline to \sim

18 mag after 80 ks. They concluded that the GRB 191221B optical afterglow is powered by slow-cooling synchrotron emission, ruling out a reverse-shock origin.

3.13. Very small satellites for multifrequency astrophysics

I do not want to enter in a discussion about small (and very small) satellites. However, I suggest to the reader to see the fundamental paper "*Small satellites for space science: A COSPAR scientific roadmap*" by Millan et al. (2019) in which there are the recommendations to: (i) the science community; (ii) the space industry; (iii) the space agencies; (iv) the policy makers; (v) the COSPAR.

A fundamental paper about "*Global Trends in Small Satellites*" discussed about the future of small satellites (smallsats) starting about their definition. Indeed, there is no universally accepted definition of a small satellite. Various groups and reports have classified smallsats according to their mass, volume, cost, capabilities, or some combination thereof. A reasonable compromise defines smallsats as satellites with masses < 200 kg. However, some exceptions are possible (Lal et al., 2017).

The global consultancy Euroconsult predicts that, whereas fewer than 700 smallsats were launched from 2006-2015, up to 3,600 smallsats are likely to be launched in the coming decade for a variety of missions. This number could reach well over 10,000 if even a fraction of the planned broadband constellations are deployed. This fact pose a problem about the overcrowding and debris concerns, especially for the Low Earth Orbits (LEO). This renders unsafe satellite operation in LEO orbits. In this scenario, as a result of the growing number of smallsats in LEO and one or more high debris-causing collisions, it is unsafe to operate satellites in orbits between 500 and 1,200 km without risking collision. As a consequence, LEO is no longer viable for widespread commercialization without government reimbursement. Further, smallsats are larger and more expensive for operation in different orbits. Smallsats operating in higher orbits have an increased cost to manufacture, given the need for radiation and higher power, and are more costly to launch and operate (Behrens & Lal, 2019).

About the use in astronomy of very small satellites see the presentation *CubeSats in astronomy and astrophysics* by Cahoy (2015), where a panorama of the potential use of these Cubesats for enhancing the knowledge of many problems in different fields of astrophysics is discussed.

An interesting paper critically discuss the opportunities for astrophysics of using smallsats, from Radio-, to Infrared- to HE-astronomy until the hunt to exoplanets and the "mystery" of solar system, by studying the astrobiology involved in (Serjeant, Elvis & Tinetti, 2020). The potential science questions are indeed both biological and chemical. And finally smallsats are often used to increase the Technology Readiness Level (TRL) of a satellite component by demonstrating capability in an operational environment. All these future possibilities are becoming real as the cost and technical barriers to smallsat-astronomy are reduced, one possible overarching consequence of increasing the numbers of PI-led

missions is the impact on and from Open Science. Observatory missions typically have raw data proprietary lifetimes of 6-12 months, while PI missions and instruments sometimes have much more restrictive policies. Initiatives such as the European Open Science Cloud (Ayrís et al., 2016) aim to make all data FAIR (Findable, Accessible, Interoperable, Reusable), which in astronomy usually involves, among other things, the integration of products into the Virtual Observatory (Pasian et al., 2016). Meanwhile, data management and deposition plans are increasingly being required by funding bodies. Commissioning novel instrumentation can sometimes be a sound justification for extended proprietary lifetimes, but existing software, data standards and data repositories can still represent a significant cost saving to a small mission. The future smallsat-astronomy community could therefore do well to maintain the open data culture from observatories, not just for exploiting existing standards and repositories, but also for teams to be eligible for follow-on funding in the current climate of open data.

4. Conclusions

I believe this review article is helpful in illustrating the impact of using robotic telescopes on advancing knowledge about our Universe. In fact, their contribution ranges from the various fields of "classical" astrophysics to the discovery of exoplanets which constitutes one of the most fascinating themes of current research. Undoubtedly, the advantages of robotic telescopes are much greater than the technical difficulties of their use. Indeed, with networks of robotic telescopes spread across the globe at all longitudes and latitudes, surveys of cosmic sources can be made seamlessly. This implies a deeper understanding of the physical phenomena occurring in the target sources.

Because of a reasonable length of this paper, I have been obliged to make a strong selection of the arguments discussed, that however are, in my opinion, sufficient to demonstrate the importance of the results obtained with different networks of robotic telescopes.

Acknowledgments. This research has made use of The NASA's Astrophysics Data System.

References

- Abbott, B.P. et al. (LIGO Scientific Coll. and Virgo Coll.): 2017a, PhRvL 119, Issue 16, id. 161101
- Abbott, B.P. et al. (LIGO Scientific Collaboration and Virgo Collaboration, Fermi GBM, INTEGRAL, IceCube Collaboration, AstroSat Cadmium Zinc

Telluride Imager Team, IPN Collaboration, The Insight-HXMT Collaboration, ANTARES Collaboration, The Swift Collaboration, AGILE Team, The 1M2H Team, The Dark Energy Camera GW-EM Collaboration and the DES Collaboration, The DLT40 Collaboration, GRAWITA: GRAvitational Wave Inaf TeAm, The Fermi Large Area Telescope Collaboration, ATCA: Australia Telescope Compact Array, ASKAP: Australian SKA Pathfinder, Las Cumbres Observatory Group, OzGrav, DWF (Deeper, Wider, Faster Program), AST3, and CAASTRO Collaborations, The VINROUGE Collaboration, MASTER Collaboration, J-GEM, GROWTH, JAGWAR, Caltech-NRAO, TTU-NRAO, and NuSTAR Collaborations, Pan-STARRS, The MAXI Team, TZAC Consortium, KU Collaboration, Nordic Optical Telescope, ePESSTO, GROND, Texas Tech University, SALT Group, TOROS: Transient Robotic Observatory of the South Collaboration, The BOOTES Collaboration, MWA: Murchison Widefield Array, The CALET Collaboration, IKI-GW Follow-up Collaboration, H.E.S.S. Collaboration, LOFAR Collaboration, LWA: Long Wavelength Array, HAWC Collaboration, The Pierre Auger Collaboration, ALMA Collaboration, Euro VLBI Team, Pi of the Sky Collaboration, The Chandra Team at McGill University, DFN: Desert Fireball Network, ATLAS, High Time Resolution Universe Survey, RIMAS and RATIR, and SKA South Africa/MeerKAT): 2017b, ApJL 848, Issue 2, article id. L12, 59 pp.

Akerlof, C. et al.: 2000, AJ 119, Issue 4, 1901-1913.

Akerlof, C.W. et al.: 2003, PASP 115, Issue 803, 132-140. .

Albrow, M. et al.: 1996, in *Astrophysical applications of gravitational lensing*, C.S. Kochanek & Jacqueline N. Hewitt (Eds.), IAU Symp. 173, Kluwer Academic Publishers; Dordrecht, pp. 227-228.

Albrow, M. et al.: 1998, ApJ 509, Issue 2, 687-702.

Allan, A. et al.: 2004, in *Advanced Software, Control, and Communication Systems for Astronomy*. Lewis, Hilton, Raffi, Gianni (Eds.), Proc. of the SPIE 5496, 313-322.

Allan, A., Naylor, T., Saunders, E.S.: 2006, Astron. Nach. 327, Issue 8, p.767

Ayris, P. et al.: 2016, *Realising the European Open Science Cloud*, Publ. Office of the European Union, Luxembourg.

Batista, V.: 2018, in *Handbook of Exoplanets*, ISBN 978-3-319-55332-0. Springer International Publishing AG, part of Springer Nature, 2018, id. 120.

Behrens, J.R., Lal, B.: 2019, New Space 7, issue 3, 126-136.

Bennett, D. et al.: 2019, in *Astro2020: Decadal Survey on Astronomy and Astrophysics*, science white papers, no. 505; Bulletin of the AAS 51, Issue 3, id. 505.

Blackman, J.W et al.: 2021, Nature 598, Issue 7880, 272-275.

- Bloom, J., Castro-Tirado, A.J., Hanlon, L., Kotani, T. (Eds.): 2010, *I Workshop on Robotic Autonomous Observatories*, Advances in Astronomy, Vol. 2010.
- Bond, I.A. et al.: 2017, MNRAS 469, Issue 2, 2434-2440.
- Boroson, T. et al.: 2014, Proc. of the SPIE 9149, id. 91491E, 10 pp.
- Bredall, J.W. et al.: 2020, MNRAS 496, Issue 3, 3257-3269.
- Brown, T.M. et al.: 2013, PASP, 125, Issue 931, 1031-1090.
- Brown, A. et al.: 2018, in *The 20th Cambridge Workshop on Cool Stars, Stellar Systems and the Sun*, Online at <http://coolstars20.cfa.harvard.edu/>, cs20, id. 28.
- Buckley, D., 2015, talk at the Palermo Workshop on " *The Golden Age of Cataclysmic Variables and Related Objects - III*".
- Buckley, D.A.H. et al.: 2021, MNRAS 506, Issue 3, 4621-4631.
- Caballero-García, M.D. et al.: 2014, in *10 Years of Discovery (SWIFT 10)*, Online at <http://pos.sissa.it/cgi-bin/reader/conf.cgi?confid=233>, id. 126.
- Caballero-García, M.D. et al.: 2015, MNRAS 452, Issue 4, 4195-4202.
- Caballero-García, M.D., Pandey, S.B., Hiriart & Castro-Tirado, A.J. (Eds.): 2016, *IV Workshop on Robotic Autonomous Observatories*, RMxAC Vol. 48.
- Caballero-García, M.D. et al.: 2016, in *IV Workshop on Robotic Autonomous Observatories*, María Dolores Caballero-García, Shasi B. Pandey, David Hiriart & Alberto J. Castro-Tirado (Eds.), Rev. Mex. A&A, (Serie de Conferencias) Vol. 48, 59-63.
- Caballero-García, M.D., Pandey, S.B. & Castro-Tirado, A.J. (Eds.): 2019, *V Workshop on Robotic Autonomous Observatories*, RMxAC Vol. 51.
- Cahoy, K.: 2015, Presentation at the SSB CubeSat Symposium, Irvine, CA, 2 September 2015. Online at http://sites.nationalacademies.org/cs/groups/ssbsite/documents/webpage/ssb_167819.pdf
- Castro-Tirado, A.J. et al.: 1999, A&A Suppl. Ser. 138, 583-585.
- Castro-Tirado, A.J. et al.: 2000, in *Gamma-Ray Bursts*, AIP Conf. Proc. 526, 260-264.
- Castro Cerón, J.M.: 2011, talk at the Frascati Workshop 2011 on " *Multifrequency Behaviour of High Energy Cosmic Sources*".
- Castro-Tirado, A.J.: 2008, in *3rd Symposium of the Astrophysics Group of the Spanish Royal Physical Society (RSEF)*, A. Ulla & M. Manteiga (Eds.), Lecture Notes and Essays in Astrophysics 3, 131.
- Castro-Tirado, A.J.: 2010a, Adv. Astron. 2010, Article ID 570489, 8 pp.
- Castro-Tirado, A.J.: 2010b, Adv. Astron. Vol. 2010, Article ID 824731, 1 p.

- Castro-Tirado, A.J. et al.: 2012, in *Second Workshop on Robotic Autonomous Observatories*, Sergey Guziy, Shashi B. Pandey, Juan C. Tello & Alberto J. Castro-Tirado (Eds.), ASI Conf. Ser. 7, 313-320.
- Castro-Tirado, A.J. Pandey, S.B. & Caballero-García (Eds.): 2021, *VI Workshop on Robotic Autonomous Observatories*, RMxAC Vol. 53.
- Cui, X.H. et al.: 2014, ApJ 795, Issue 2, article id. 103, 6 pp.
- Deeg, H.J., Alonso, R.: 2018, in *Handbook of Exoplanets*, ISBN 978-3-319-55332-0. Springer International Publishing AG, part of Springer Nature, 2018, id. 117.
- Dominik, M. et al.: 2004, in *Extrasolar planets: Today and Tomorrow*, J.-P. Beaulieu, A. Lecavelier des Etangs, & C. Terquem (Eds.), ASP Conf. Ser. 321, 121-122.
- Edwards, B. et al.: 2021, Astron. Theory, Observ. and Meth. J. 1, No. 1, 1-12. Also arXiv:2111.10350.
- Eyer, L.: 1999, Baltic Astron. 8, 321-324.
- Eyer, L., Cuypers, J.: 2000, in *The Impact of Large-Scale Surveys on Pulsating Star Research*, L. Szabados & D. Kurtz (Eds.), ASP Conf. Ser. 203, 71-72.
- Fujiwara, T. et al.: 2017, in *7 years of MAXI: monitoring X-ray Transients*, held 5-7 December 2016 at RIKEN. Online at <https://indico2.riken.jp/indico/conferenceDisplay.py?confId=2357>, p. 277.
- Gandhi, P. et al.: 2016, MNRAS 459, Issue 1, 554-572.
- Gao, H. et al.: 2015. ApJ 810, Issue 2, article id. 160, 13 pp.
- Gaudi, B.S et al.: 2002, ApJ 566, Issue 1, 463-499.
- Giovannelli, F.: 2016, in *Proceedings of the 4th Ann. Conf. on High Energy Astrophysics in Southern Africa (HEASA 2016)*. Online at <http://pos.sissa.it/cgi-bin/reader/conf.cgi?confid=275>, id. 31.
- Gorbovskoy, E.S. et al.: 2016, MNRAS 455, 3312-3318.
- Guziy, S., Pandey, S.B., Tello, J.C. & Castro-Tirado, A.J. (Eds.): 2012, *II Workshop on Robotic Autonomous Observatories*, Astron. Soc. of India Conf. Ser., Vol. 7.
- Guziy, S. et al.: 2013, in *Gamma-ray Bursts: 15 Years of GRB Afterglows*. A.J. Castro-Tirado, J. Gorosabel & I.H. Park (Eds.), EAS Publ. Ser. 61, 251-254.
- Hamuy, M. et al.: 2006, PASP 118, Issue 839, 2-20.
- Hamuy, M. et al.: 2012, Mem. S.A.It. Vol. 83, 388.
- Herald, A. et al. (OGLE Coll.; MOA Coll.; The Spitzer Team; The MiNDSTEP Consortium; The LCO & μ FUN Coll.): 2022, arXiv:2203.04034.

- Hermes, J.J.: 2018, in *Handbook of Exoplanets*, ISBN 978-3-319-55332-0. Springer International Publishing AG, part of Springer Nature, 2018, id. 6.
- Hessman, F.V.: 2001a, in *Small Telescope Astronomy on Global Scales*, Bohdan Paczynski, Wen-Ping Chen & Claudia Lemme (Eds.), ASP Conf. Ser. 246, 13.
- Hessman, F.V.: 2001b, in *Small Telescope Astronomy on Global Scales*, Bohdan Paczynski, Wen-Ping Chen & Claudia Lemme (Eds.), ASP Conf. Ser. 246, 357.
- Hidas, M.G. et al.: 2008, *Astron. Nach.* 329, Issue 3, 269-270.
- Hirao, Y. et al. (The MOA Coll.; The OGLE Coll.): 2017, *AJ* 154, Issue 1, article id. 1, 8 pp.
- Hirao, Y. et al. (The OGLE Coll.; The KMTNet Coll.; The Spitzer Team; The LCO and μ FUN Follow-up Teams; The MindSTeP Coll.; The IRSF Team): 2020, *AJ* 160, Issue 2, id. 74.
- Hudec, R. et al.: 2017, talk at the Frascati Workshop 2017 on *Multifrequency Behaviour of High Energy Cosmic Sources - XII*, Mondello, Palermo, Italy, 12-17 June.
- Jordana-Mitjans, N. et al.: 2020, *ApJ* 892, Issue 2, id. 97, 17 pp.
- Jung, Y.K. et al.: 2020a, *AJ* 160, Issue 3, id. 148, 18 pp.
- Jung, Y.K. et al.: 2020b, *AJ* 160, Issue 6, id. 255, 11 pp.
- Kokori, A. et al.: 2021, *Experimental Astronomy*, Online First at <https://doi.org/10.1007/s10686-020-09696-3>.
- Kreitzer, M.H.: 1976, *Image Quality Criteria for Aberrated Systems*, PhD Thesis, The University of Arizona (USA), Source: Dissertation Abstracts International, Volume: 37-09, Section: B, page: 4538.
- Kramer, M.: 2018, in *Handbook of Exoplanets*, ISBN 978-3-319-55332-0. Springer International Publishing AG, part of Springer Nature, 2018, id. 5.
- Lal, B. et al.: 2017, IDA SCIENCE & TECHNOLOGY POLICY INSTITUTE, Paper P-8638; Log: H 17-000435.
- Lam, C.Y. et al.: 2022, arXiv:2202.01903.
- Lazio, T.J.W.: 2018, in *Handbook of Exoplanets*, ISBN 978-3-319-55332-0. Springer International Publishing AG, part of Springer Nature, 2018, id. 9.
- Liang, En-Wei et al.: 2010, *ApJ* 725, Issue 2, 2209-2224.
- Lipunov, V.M.: 1987, *Ap&SS* 132, no. 1, 1-51.
- Lipunov, V.M.: 1995, in *Frontier Objects in Astrophysics and Particle Physics*, F. Giovannelli & G. Mannocchi (Eds.), SIF, Bologna, Italy, 47, 61-76.

- Lipunov, V.M., Postnov, K.A., Prokhorov, M.E.: 2001, ARep 45, Issue 3, 236-240.
- Lipunov, V.M., Postnov, K.A.: 1988, Ap&SS 145, no. 1, 1-45.
- Lipunov, V., Kornilov, V. et al.: 2010, Adv. Astron. article id. 349171, 6 pp.
- Lipunov, V.M. et al.: 2016a, ApJ 833, Issue 2, article id. 198, 12 pp.
- Lipunov, V.M. et al.: 2016b, MNRAS 455, 712-724.
- Lipunov, V.M. et al.: 2017a, MNRAS 470, 2339-2350.
- Lipunov, V.M. et al.: 2017b, MNRAS 465, 3656-3667.
- Lipunov, V.M. et al.: 2017c, New Astron. 51, 122-127.
- Lipunov, V.M. et al.: 2017d, ApJL 850, Issue 1, article id. L1, 9 pp.
- Lipunov, V.M. et al.: 202, ApJL 896, Issue 2, id. L19, 5 pp.
- Liu, C-J., Zhen Yao, Z., Ding, W-B.: 2017, Res. Astron. Astrophys. 17, No. 8, 78 (10 pp).
- Malbet, F., Sozzetti, A.: 2018, in *Handbook of Exoplanets*, ISBN 978-3-319-55332-0. Springer International Publishing AG, part of Springer Nature, 2018, id. 196.
- Markwardt C.B. et al.: 2015, GRC Circ., 17688, 1.
- Marshall, S. et al.: 1997, AAS 191st AAS Meeting, id. 48.15; Bulletin of the AAS Vol. 29, p. 1290.
- Millan, R.M. et al.: 2019, Adv. Spa. Sci. 64, Issue 8, 1466-1517.
- Monard, L.A.G.: 2008, CBET 1315.
- Moskovich, J.: 1978, in *Computer-Aided Optical Design*, R.E. Fischer. Bellingham, WA (Eds.), SPIE Proc. Vol. 147. Society for Photo-Optical Instrumentation Engineers, p. 149.
- Pasian, F. et al.: 2016, *ASTERICS: Addressing Cross-Cutting Synergies and Common Challenges for the Next Decade Astronomy Facilities*, in *Astronomical Data Analysis Software and Systems XXV* 512, 57-60.
- Pastorello, A. et al.: 2019, VizieR On-line Data Catalog: J/MNRAS/453/3649. Originally published in: 2015MNRAS.453.3649P.
- Pignata, G. et al.: 2009, AIPC, 1111, 551.
- Planck Collaboration; Ade, P.A.R. et al.: 2016, A&A 594, id. A13, 63 pp.
- Pueyo, L.: 2018, in *Handbook of Exoplanets*, ISBN 978-3-319-55332-0. Springer International Publishing AG, part of Springer Nature, 2018, id. 10.
- Quimby, R.M. et al.: 2012, AJ 144, Issue 6, article id. 177, 16 pp.
- Rabaza, O. et al.: Rev. Sci. Instr. 84, Issue 11, id. 114501-114501-9.

- Ranc, C.: 2015a, Ph.D. Thesis, Institut d'Astrophysique de Paris, Université Pierre et Marie Curie - Paris VI, 326 pages.
- Ranc, C. et al.: 2015b, A&A 580, id. A125, 16 pp.
- Ranc, C. et al.: 2021, MNRAS 506, Issue 1, 1498-1506.
- Ruiz-Velasco, A.E. et al.: 2007, ApJ 669, Issue 1, 1-9.
- Sackett, P.N. et al.: 2003, in *Bioastronomy 2002: Life Among the Stars*, R. Norris, C. Oliver & F. Stootman (Eds.), IAU Symp. 213, ASP Conf. Ser. TBD, 1-5.
- V. A. Sadovnichy, V.A. et al.: 2018, ApJ, 861, Issue 1, article id. 48, 12 pp.
- Schaefer, B.E., King, J.R., Deliyannis, C.P.: 2000, ApJ 529, Issue 2, 1026-1030.
- Schreiber, M.R. et al.: 2019, ApJL 887, Issue 1, article id. L4, 8 pp.
- Serjeant, S., Elvis, M., Tinetti, G.: 2020, Nature Astron. 4, 1031-1038.
- Shimokawabe, T. et al.: 2009, AIPC 1133, 79.
- Shin, In-Gu et al.: 2022, arXiv:2201.04312.
- Sicilia-Aguilar, A. et al.: 2017, A&A 607, id. A127, 27 pp.
- Singh, M. et al.: 2019, MNRAS 485, Issue 4, 5438-5452.
- Skowron, J. et al. (The OGLE Coll.; The MOA Coll.; The Wise group; The μ FUN Coll.; The PLANET Coll.; The RoboNet Coll.; The MiNDSTEp consortium): 2015, ApJ 804, Issue 1, article id. 33, 12 pp.
- Slowikowska, A., et al.: 2016, MNRAS 458, Issue 1, 759-771.
- Tachibana, Y., Kawai, N., Pike, S. (for the MAXI team and the MITSuME team): 2015, in *5th Fermi Symposium Proc.: Nagoya, Japan: 20-24 Oct, 2014*, arXiv:1502.03610.
- Tachibana, Y. et al.: 2017, PASJ 69, Issue 4, id. 63.
- Tachibana, Y. et al.: 2018, PASJ 70, Issue 5, id. 92.
- Tanvir, N.R. et al.: 2009, Nature 461, Issue 7268, 1254-1257.
- Tello, J.C., Riva, A., Hiriart, D. & Castro-Tirado, A.J. (Eds.): 2014, *III Workshop on Robotic Autonomous Observatories*, RMxAC, Vol. 45.
- Tsapras, Y. et al.: 2009, Astron. Nachr. 330, No. 1, 4-11.
- Valenti, S. et al.: 2014, MNRAS 438L, Issue 1, L101-L105.
- Valenti, S. et al.: 2015, ApJL 813, Issue 2, article id. L36, 5 pp.
- Van Dyk, S.D. et al.: 2012, AJ 143, Issue 1, article id. 19, 12 pp.
- Vestrand, W.T. et al.: 2002, in *Advanced Global Communications Technologies for Astronomy II*, Kibrick, Robert I (Ed.), Proc. of the SPIE 4845, 126-136.
- Voges, W. et al.: A&A 349, 389-405.

- Watson, M.G.: 2003, in *Astronomical Data Analysis Software and Systems XII*, H.E. Payne, R.I. Jedrzejewski & R.N. Hook (Eds.), ASP Conf. Ser. 295, 107-116.
- White, R.R. et al.: 2004, in *Advanced Software, Control, and Communication Systems for Astronomy*. Lewis, H., Raffi, G. (Eds.), Proc. of the SPIE, Vol. 5496, 302-312.
- Woźniak, P.R. et al.: 2002, in *Virtual Observatories*, Szalay, Alexander S (Ed.), Proc. of the SPIE 4846, 147-157.
- Woźniak, P.R. et al.: 2004, AJ 127, Issue 4, 2436-2449.
- Wright, J.T.: 2018, in *Handbook of Exoplanets*, ISBN 978-3-319-55332-0. Springer International Publishing AG, part of Springer Nature, 2018, id. 4.
- Yee, J.C. et al.: 2018, arXiv:1803.07921.
- Yee, J.C. et al.: 2021, AJ 162, Issue 5, id. 180, 22 pp.
- Yost, S.A. et al.: 2006, Astron. Nach. 327, Issue 8, p. 803.
- Zang, W. et al.: 2020, arXiv:2010.08732.
- Zang, W. et al.: 2021a, AJ 162, Issue 4, id. 163, 18 pp.
- Zang, W. et al.: 2021b, Res. A&A 21, Issue 9, id. 239, 19 pp.